



Project acronym and title:
SECURE – Subsurface Evaluation of Carbon capture
and storage and Unconventional risks

**REPORT ON THE EXPERIMENT-BASED
KNOWLEDGE ON ACOUSTIC EMISSION
CHARACTERISTICS OF CCS AND SHALE GAS
OPERATIONS AND SUGGESTIONS ON HOW TO
MITIGATE SEISMICITY FOR BOTH**

Authors and affiliation:
Pierre Cerasi

SINTEF AS - SINTEF Industry, S. P. Andersens vei 15 B, 7031, Trondheim, Norway

Email of lead author:
pierre.cerasi@sintef.no

D5.2
Revision:1

Disclaimer

This report is part of a project that has received funding by the *European Union's Horizon 2020 research and innovation programme* under grant agreement number 764531.

The content of this report reflects only the authors' view. The *Innovation and Networks Executive Agency (INEA)* is not responsible for any use that may be made of the information it contains.



Project funded by the European Commission within the Horizon 2020 Programme

Dissemination Level

PU *Public* x

Deliverable number:	D5.2
Deliverable name:	Report on the experiment-based knowledge on acoustic emission characteristics of ccs and shale gas operations and suggestions on how to mitigate seismicity for both
Work package:	5 Impact Mitigation and Remediation
Lead WP/deliverable beneficiary:	SINTEF AS/ SINTEF AS

Status of deliverable		
	By	Date
Submitted (Author(s))	Pierre Cerasi	24.09.2019
Verified (WP leader)	Pierre Cerasi	
Approved (EB member)	Jonathan Pearce	07/10/19
Approved (Coordinator)		

Author(s)		
Name	Organisation	E-mail
Pierre Cerasi	SINTEF AS - Industry	Pierre.cerasi@sintef.no



Public introduction

Subsurface Evaluation of CCS and Unconventional Risks (SECURE) is gathering unbiased, impartial scientific evidence for risk mitigation and monitoring for environmental protection to underpin subsurface geoenergy development. The main outputs of SECURE comprise recommendations for best practice for unconventional hydrocarbon production and geological CO₂ storage. The project is funded from June 2018–May 2021.

The project is developing monitoring and mitigation strategies for the full geoenergy project lifecycle; by assessing plausible hazards and monitoring associated environmental risks. This is achieved through a program of experimental research and advanced technology development that includes demonstration at commercial and research facilities to formulate best practice. We will meet stakeholder needs; from the design of monitoring and mitigation strategies relevant to operators and regulators, to developing communication strategies to provide a greater level of understanding of the potential impacts.

The SECURE partnership comprises major research and commercial organisations from countries that host shale gas and CCS industries at different stages of operation (from permitted to closed). We are forming a durable international partnership with non-European groups; providing international access to study sites, creating links between projects and increasing our collective capability through exchange of scientific staff.

Executive report summary

The aim of Work Package 5 (WP5) in the SECURE project is to establish best practices for remedial and mitigation technologies and strategies which would reduce risk for shale gas and CO₂ storage operations. Several potential remediation technologies have been identified and their suitability and effectiveness for risks associated with geoenergy operations are being assessed.

This report reviews Acoustic Emission (AE) laboratory tests designed to investigate mechanisms by which micro-seismicity arises in CCS and shale gas operations. The differences between the two subsurface operations are reviewed, in terms of the stress path leading to rock failure and acoustic emission. This in turn leads to different methodologies for laboratory set-up and test design:

- (1) Shale gas operations: these are characterised by fracturing of low-permeability rocks to create conduits for the gas to flow to the production well. Seismicity arises primarily with the fracturing operation; this can be used to monitor growth of multiple fractures in a multi-stage operation, but is not readily duplicated in laboratory tests. Instead, experimentation looks at reproducing a single fracturing event and exploring the mechanisms at work from the pore size level and up. The energy distribution as event intensity increases can be recorded and can be potentially used for monitoring purposes in the field, indicating induced stress level and operation conformance with plans. The challenges in the laboratory are related to creating a hydraulic fracture that can be monitored without it destroying the specimen and surrounding instrumentation, at least not before any useful data recording can be performed.*

CCS operations: hydraulic fracturing is to be avoided in such operations. Any recorded passive seismicity is therefore assumed to arise further inside the reservoir, or from the overburden or underburden. AE is mostly then arising due to reactivation of small faults, critically stressed and favourably oriented as the pressure plume from the injected CO₂ passes the fault. The assumed mechanism generating AE is increase of pore pressure, with shear stress leading to sliding on a critically oriented fault. This is also possible to investigate in the laboratory, provided the in-situ stress state can be approximated by biaxial conditions or where a triaxial cell with pore pressure control is available. Examination of the energy distribution together with triangulation to localise the origin of the emission may be an indicator of the reactivation of sub-seismic faults.



Contents

Public introductionii

Executive report summary.....ii

Contentsiii

1 Introduction5

2 Acoustic emission tests in the laboratory6

 2.1 experiments targeting shale gas operations.....7

 2.2 experiments targeting CCS operations9

 2.3 Planned tests in the SECURE project 13

3 Recommendations for mitigating seismicity 13

4 Conclusions..... 14

5 References..... 15

FIGURES

Figure 1. Instrumentation around a sleeved core plug (deformation gauges and ultrasonic transducers) ..6

Figure 2. Example of triaxial cells at the SINTEF Formation Physics laboratory. Left: Triaxial loading frame made by MessTek Prüfsysteme GmbH; right: triaxial loading frame made by TerraTek, a Schlumberger Company.6

Figure 3. True triaxial load frames allowing for 3 different applied stress components. Left: University of Pittsburgh; right: SINTEF.7

Figure 4. Three different possible interactions between a hydraulic fracture from an injection well and a natural fracture in its vicinity. Left: the triggered fracture is arrested by the natural fracture (inflating it or possibly reactivating it); middle: the triggered fracture traverses the natural fracture; right: the triggered fracture is deviated by the natural fracture.7

Figure 5. Illustration of the finite specimen size effect, where a fracture reaches the outer boundary of the tested plug. Here, erosion under inward radial flow in high confining stress conditions is seen to propagate all the way to the sandstone plug's outer surface. Examples from sand production tests at SINTEF on Castlegate outcrop sandstone (left and middle, photographs after testing and right, CT scan cross sections along the plug's axis).8

Figure 6. Timeline of fracture creation and reactivation on Mount Simon sandstone specimen..... 10

Figure 7. Reactivation of the fracture in a small sample test on Castlegate sandstone. Significant increase in AE is seen (red dots) as the pore pressure is increased (blue line) while the applied stresses are kept constant. 10

Figure 8. Different scaling law for fracturing and reopening, compared to sliding of fracture. 11

Figure 9. Localisation of AE events in Mt. Simon sandstone (left) and Castlegate outcrop (right). 11

Figure 10. Micro-CT image reconstruction isolating the fracture planes detected in the two sandstone specimens with stress-induced fractures. Left: Mt. Simon sandstone; right: Castlegate sandstone. . 12



Figure 11. Left: Castlegate sandstone plug cut in two parts, reassembled in the triaxial cell to form a pre-existing fracture. Typical test result (no AE recorded) showing reactivation only happened for high deviatoric stress and high pore pressure increase (large drop/increase in radial/axial strain). 12

Figure 12 Schematic illustration of planned fracturing experiments to test remediation fluid placement and property evaluation. At left: a shale core with a partially cemented borehole section is fractured by pressurising the borehole. Right: geometry of the assembly showing the cement sheath covering part of the internal surface area of the borehole. 14

TABLES

No table of figures entries found.



1 Introduction

Subsurface operations related to energy production such as oil and gas, geothermal wells and mining of coal and minerals, as well as CO₂ injection, are often accompanied by sudden rock straining, which releases acoustic energy in the form of seismicity, felt or measured at the surface (Lockner, 1993). In oil and gas production, this microseismicity can occur both during primary production and when injecting fluids for secondary or tertiary recovery (enhanced oil or gas recovery). During production, microseismicity has been linked to subsidence; the source of the energy emission probably originates from stress arching and concentration at points around the flanks of the reservoir, either activating bounding faults or initiating shear failure in the caprock itself (Smith *et al.*, 2017). In injection operations, water or CO₂ causes transient pressure increase in the reservoir, which can trigger slippage of small faults in the reservoir itself or again, in the caprock or basement formation (Cerasi *et al.*, 2018). In unconventional oil and gas operations, the practice of deliberately inducing hydraulic fractures is common for onshore shale plays, where the matrix permeability is too low to allow for traditional production strategies. The multiple fractures triggered by increasing the well pressure above the threshold causing the effective hoop stress to exceed the tensile strength of the shale formation, creates an assembly of parallel, high permeability drainage paths to the well (Cheng, 2012). The hydraulic fracturing operation inevitably leads to microseismicity, related to energy emission upon tensile opening and further propagation of the fractures away from the well. In subsurface mining, straining of tunnel roofs between pillars can generate stress concentrations leading to AE (acoustic emission), or again, reactivation and slippage of a fault crossing the mine (Szwedzicki, 2001).

Where this microseismicity gets measured, the magnitude of surface acceleration is used as a traffic light monitoring scheme, whereby threshold values initiate corrective measures or shut-down of operations (Butcher *et al.*, 2017). However, the same monitoring scheme can also be used to evaluate conformance of operations to plans and models of the subsurface; thus, the extent of individual fractures in a multistage fracturing operation can be assessed, or the extent of an injected CO₂ plume evaluated as it progresses in the underground (Eliasson *et al.*, 2018). Correct measurement and interpretation of AE requires knowledge of the subsurface in terms of lithology sequence, formation properties, presence and orientation of faults and natural fractures and nucleation position of acoustic energy generation. All this information is difficult to acquire, and accuracy increases with increasing the number of monitoring wells, seismic surface sensors and types of downhole and surface captors (such as tiltmeters, multi-component accelerometers deployed down-hole, optic fibre captors etc.). Even when a rich suite of measurements is acquired, interpretation of the data remains dependent on having good and suitable models for the area, notably for the mechanical properties of the rocks, acoustic velocity as a function of stress and anisotropy, attenuation characteristics, fault sealing properties, cohesion and friction properties (Goertz-Allmann *et al.*, 2017).

Laboratory experimental campaigns, if possible on relevant field cores, are therefore invaluable aids, primarily in calibration of models for the area considered. These can shed light on localisation of AE sources, correcting sometimes early interpretation of underground events leading to microseismicity occurrence and suggesting corrective action, such as injection rate reduction, or even (limiting ourselves here to shale gas and CCS operations). In general, however, more fundamental research is still needed to help interpret hypotheses about fundamental aspects of microseismicity, such as micro-crack formation, failure mode, coalescence of larger fractures, sliding of fracture zones versus stick-slip motion and the relation of all these preceding components with the prediction of energy measurements at given locations. In particular, it remains unclear as to what leads to seismic as opposed to aseismic events; seismic events are micro-fractures or stick-slip movements of faults rapidly dissipating energy in the form of acoustic energy, with sudden short local acceleration propagating as waves outwards. Aseismic events refer to slip along a fault plane, without acoustic energy emission. It is as well unclear which formation properties (brittle as opposed to ductile, permeability, saturation fluid and extent, fabric anisotropy etc.) are conducive to large seismicity for given scenarios, how and to what extent topography of layers and stiffness contrasts promote AE. These questions can only begin to be answered in bespoke experiments, isolating in the best possible way the properties or mechanisms for a given scenario being tested. Thus, simplification may be made by using outcrop rocks with known properties, simulated faults with saw-cut versus stress-induced fractures, where the surface properties such as roughness are well measured, controlled fluid saturation and simplified stress paths (Cerasi *et al.*, 2018).



2 Acoustic emission tests in the laboratory

Experiments to record acoustic emission in rocks usually make use of conventional triaxial cells (in reality, biaxial as opposed to so-called true triaxial), where cylindrical rock specimens are inserted in a pressure vessel to apply confining stress through a rubber membrane, jacketing the rock itself (Figure 1). This pressure vessel is then introduced into a load frame, such that a piston can be made to apply additional axial force on the specimen and allow for complex stress paths to be applied to the tested rock (Figure 2). The triaxial cell is instrumented with strain gauges giving a full set of deformation measurements (axial and radial deformation, measured at multiple locations – see Figure 1). In addition, a set of piezoelectric transducers is appended to the specimen sleeve, so as to record acoustic energy in multiple locations around the sample and permit triangulation for localisation of event source. These or additional crystals can be used to also actively send acoustic pulses in different directions through the sample, to measure wave and group velocities as a function of stress level and direction, to help calibrate the localisation routine. When possible, differentiating between pressure and shear acoustic waves (V_p and V_s), gives extra clues on saturation conditions and fracture distribution and sizes, as shear waves do not propagate in liquids.

Other occasional rigs can be encountered, such as shear boxes, where a direct shear plane is imposed on the rock specimen at given normal stress and deformation rate. A variation on this is the ring shear device, permitting in essence unlimited deformation, usually more frequent in unconsolidated soil testing. True triaxial cells can also be used, but mostly without control of pore fluid pressure beyond a pure injection scheme from a drilled wellbore, for example (Figure 3).



Figure 1. Instrumentation around a sleeved core plug (deformation gauges and ultrasonic transducers).

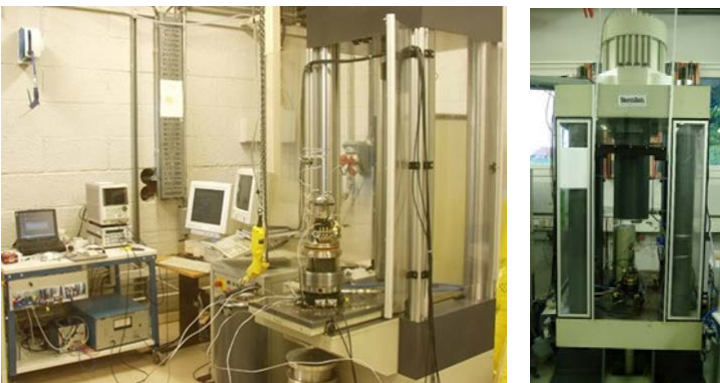


Figure 2. Example of triaxial cells at the SINTEF Formation Physics laboratory. Left: Triaxial loading frame made by MessTek Prüfsysteme GmbH; right: triaxial loading frame made by TerraTek, a Schlumberger Company.



Figure 3. True triaxial load frames allowing for 3 different applied stress components. Left: University of Pittsburgh; right: SINTEF.

An essential component for successful AE measurements is hardware and software to amplify and analyse the acoustic signal recorded in a test. A threshold in signal amplitude needs to be judiciously set so as not to saturate the recording device with continuous signal; at the same time, too low a threshold will filter out many events which could be of interest in terms of the stress conditions when they occur, or helpful to gather enough data to identify statistically significant trends. The hardware and especially the software used, in terms of number of allocated signal channels and memory capabilities, will be decisive in the quality of the obtained results, with more precise event localisation and energy trend recognition as a function of stress path. In particular, the capability of recording long wave trains for individual events can enable moment tensor inversion (Aker *et al.*, 2014); this in essence means that grain contact cracking as the origin for a given event can be further sorted in terms of grain movement (shear or tensile, where the grains either slide in opposite directions or separate with the opening of a crack, or come together in compression).

2.1 EXPERIMENTS TARGETING SHALE GAS OPERATIONS

These laboratory experiments are designed to investigate hydraulic fracturing of a studied rock specimen, in sufficiently controlled conditions that meaningful acoustic data can be gathered. However, broader investigation motivations such as seismology, where tectonic slip across faults is investigated, are also of high relevance for shale gas operations. This is due to complications due to the presence of natural fractures, which interact or interfere with the planned triggered fractures from the pressurised well (Dahi-Taleghani & Olson, 2011; Chen *et al.*, 2014), as show in Figure 4. The biggest challenge in designing hydraulic fracturing tests is the high propagating velocity of the fractures, exacerbated in the typically small dimensions used for rock plugs in traditional triaxial cells (usually a cylinder not larger than 2" diameter and 4" height). Another complicating factor is that if or when the induced fracture reaches the outer boundary of the specimen, a short circuit in terms of fracturing fluid is established and the outer plug surface is suddenly brought to the well's pressure, which can cause rupture of the rubber sleeve and damage to instrumentation. This situation is similar to solids production experiments in sandstone or chalk plugs, where erosion of the plug can eventually reach the outer surface, as shown in Figure 5.



Figure 4. Three different possible interactions between a hydraulic fracture (in blue) from an injection well (oval) and a natural fracture (green) in its vicinity. Left: the triggered fracture is arrested by the natural fracture (inflating it or possibly reactivating it); middle: the triggered fracture traverses the natural fracture; right: the triggered fracture is deviated by the natural fracture.

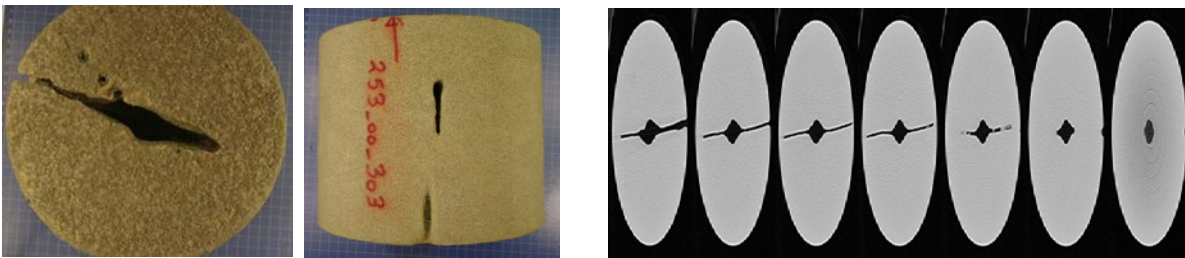


Figure 5. Illustration of the finite specimen size effect, where a fracture reaches the outer boundary of the tested plug. Here, erosion under inward radial flow in high confining stress conditions is seen to propagate all the way to the sandstone plug's outer surface. Examples from sand production tests at SINTEF on Castlegate outcrop sandstone (left and middle, photographs after testing and right, CT scan cross sections along the plug's axis).

Several attempts have been made to mitigate the above difficulties: high viscosity silicon oil or glycerol gel solution in water can be used as the fracturing fluid (Chitrala *et al.*, 2013), or simulating the hydraulic fracture without injecting fluid into the rock, separating it from the wellbore with a suitable elastic membrane (Pradhan *et al.*, 2015). Other experiments have been conducted on cubic or prismatic blocks, in biaxial or triaxial mode; these block experiments do not usually permit, as stated above, fully fluid saturated pores but only allow injection of the fracturing fluid into a dry rock. However, larger sizes can be investigated, ranging from 20 cm to 1 m face size (Matsunaga *et al.*, 1993; Oye *et al.*, 2018).

Several important features of these experiments are found which help to correlate to field observations or suggest that small scale laboratory testing can have predictive power:

- 1) Omori's scaling law, relating the frequency of aftershocks to their magnitude seems to be satisfied in laboratory experiments (Lockner, 1993),
- 2) AE energy distribution (number of counts with given energy) scales as a power law, but with specific coefficients for different rock lithology (Pradhan *et al.*, 2015),
- 3) Permeating fluid is seen to alter acoustic wave patterns recorded (Matsunaga *et al.*, 1993),
- 4) Fault reactivation depends on lubrication and is thus sensitive to fluid plume reaching the core (Oye *et al.*, 2018),
- 5) Compaction and shear bands are seen in the laboratory, corresponding to those in the field, helping confirm subsurface features from passive seismic monitoring (especially in the case of sub-seismic features, still impacting fluid flow underground) (Baud *et al.*, 2004; Fortin *et al.*, 2006),
- 6) AE from grain cement breakage scales differently from stick-slip events across existing faults, but more testing is needed to confirm finding (McLaskey & Lockner, 2016),
- 7) AE analysis in hydraulic fracturing tests shows propagation of non-planar, shear failure dominated fractures, interacting strongly with the in-situ stress field and suggesting stress-dependent fracture spacing strategy in the field (Chitrala *et al.*, 2013),
- 8) AE signature is different for shear events compared to compaction, which if upscaled to field can shed light on processes responsible for fracture propagation (Fortin *et al.*, 2009),
- 9) Increasing hydraulic fluid viscosity leads to thicker and shorter fractures, although in the laboratory further dry propagation is observed beyond the wet fracture tip (Stanchits *et al.*, 2014).

Much of the laboratory work on hydraulic fracturing has so far been performed on more permeable rocks than typical shale formations, and with considerably less fabric anisotropy (including weak planes). Studies on shales show however a strong interaction between the induced fracture and weak planes or natural fractures present in the shale, depending on the orientation of the well with respect to these intrinsic features (Wang *et al.*, 2016). These studies were however conducted dry (no injection of hydraulic fluid) on disk-shaped specimens according to the indirect tensile strength test (the Brazilian test). Other authors have investigated the relationship between the scaling of aftershocks with the size of main hydraulic fracture; keeping stress constant, further fracturing develops, accompanied by aftershocks obeying a power law, as evidenced from AE measurements during the test (Bunger *et al.*, 2015). These tests were however not in shales but were performed on impermeable crystalline rocks.

Experiments using true triaxial cells indicate that the influence of the intermediate principal stress also is very important for AE occurrence and evolution at given maximum and minimum stress values (Sun *et al.*, 2018). Fatigue effects are important as well, with AE being recorded by keeping stress levels constant but slightly



below fracturing threshold (static fatigue conditions). These tests did not involve fluid injection or saturation, being 3-point bending tests on impermeable granite (Winner *et al.*, 2018).

Unfortunately, until now, most studies have always involved injecting into dry rocks and few into anisotropic shales (Molenda *et al.*, 2015), which is not surprising, given the difficulty of obtaining intact large shale samples, due to their fissility. Another difficulty lies in the anisotropy itself, taking into account the velocity dependence on the angle between minimum and maximum values in order to make a correct localisation. Most commercial software packages make triangulation calculations using several recorded acoustic wave arrival times together with one sound velocity value, irrespective of wave path orientation with respect to the shale fabric anisotropy. A more precise localisation should be obtained by taking into account the velocity variation with ray path angle relative to bedding. This trajectory dependence of the velocity gets even more complicated by the superposed stress (path) dependence. This is due to further changes in sound velocity with increasing stress level and stress state (compressive, shear or tensile).

2.2 EXPERIMENTS TARGETING CCS OPERATIONS

Laboratory experiments of relevance to CO₂ storage investigates conditions whereby AE may be encountered without explicit fracturing of rock into which the CO₂ is injected. Indeed, CCS pilots are designed such that the maximum injection pressure never exceeds the fracturing threshold. However, injection can occur in reservoirs where bounding faults or thin shale baffles are present, but perhaps not detected due to their thin dimensions or the scarcity of nearby wells to constrain the geological model. These subsurface structures can lead to pressure buildup and potential fracturing or fracture reactivation, if injection is carried out at constant flow rate. Most operations monitor fluid pressure at the injection well and in one or more monitoring wells (Grude *et al.*, 2014), but pressure transients may arise between these measurement stations without being recorded there, or not being recorded early enough.

Maybe the most investigated case of CO₂ injection pilot microseismicity study is the IBDP injection site (Illinois Basin Decatur Project). Much research effort has been put into interpreting the recorded AE events there and comparing their occurrence with the injection schedule (Ringrose *et al.*, 2017). These events appeared in clusters, aligned roughly along the same direction and at seemingly random distance from the injection well. Calculations show that most events occurred at a distance far greater than the extent at that time of the CO₂ plume. Although the magnitude of these events never exceeded $M = 1.1$, they were unexpected taking into account the good permeability and extent of the Mount Simon sandstone reservoir, into which the CO₂ was being injected. The seismic surveys did not identify major faults compartmentalizing the sandstone, nor did any notable increase in injection pressure indicate the presence of barriers to the flow. Later studies showed that the clusters aligned with topographic features of the pre-Cambrian basement formation, and that the lower Mount Simon was highly stratified, with the presence of numerous low permeability layers above the injection horizon (Dando *et al.*, 2019). Similarly, in the Quest CCS project in Alberta, microseismic monitoring during baseline acquisition and the first years of operation did not yield a time sequence of events following the CO₂ plume outwards from the injection well (Bacci *et al.*, 2018). Rather, the events seemed randomly located and all originating from the basement rock.

Two types of experiments were attempted in the laboratory, to mimic the conditions at the IBDP site: tests on intact sandstone plugs, in which a stress-induced fracture is first generated, after which a pore pressure increase attempts to reactivate it, and tests on saw-cut sandstone plugs (Cerasi *et al.*, 2018), where the artificial fracture is attempted again to be mobilised by increasing pressure or injecting fluid (in the case where the plug is originally dry). Tests on small, cylindrical plugs with controlled pore pressure were carried out at SINTEF, while one large-scale true triaxial test with an injection borehole was carried out at Schlumberger Terratek (Oye *et al.*, 2018); all these tests were a part of the geomechanics theme of the CCS research project financed by the DoE GSCO₂ EFRC (Energy Frontier Research Center - www.gSCO2.org) at the ISGS (Illinois State Geological Survey).

The induced fracture tests showed increasing AE as the failure plane was probably forming through coalescence of microfractures, upon differential stress increase past yield shear stress but below peak shear stress. This suggests that accumulation of AE events may serve as early warning of shear fracture, which is also relevant for the shale gas case. Figure 6 shows a typical timeline for such tests, here on the Mt Simon sandstone. The red curve is the applied axial stress that is used in the first cycle to create a failure plane in the intact rock. The green curve shows the axial strain needed to reach compressive shear strength and the blue curve the pore pressure in the sandstone plug. Reopening of the fracture occurs in the second cycle, where the axial stress is kept constant somewhat below peak stress, while the pore pressure is increased, causing a jump in strain, which is interpreted as sliding of the fracture.



Associated AE events are shown in Figure 7, this time for a Castlegate outcrop plug; note that events occur both for increase of differential stress and pressure pulses. The required pulse to provoke AE becomes smaller as one nears the compressive strength limit. Sorting the emitted energy in bins seems to point to two different scaling laws (power laws of number of events at a given energy level), as shown in Figure 8. This different behaviour is only seen in experiments where large strains are recorded (pointing to slip of the fracture rather than just opening).

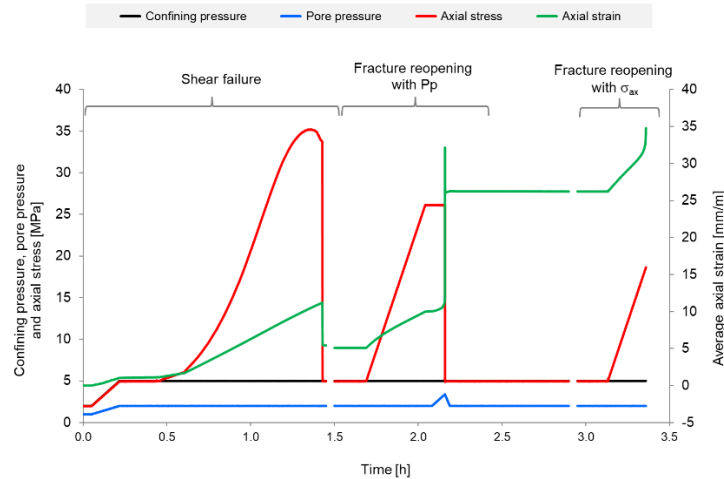


Figure 6. Timeline of fracture creation and reactivation on Mount Simon sandstone specimen (from Cerasi *et al.*, 2018).

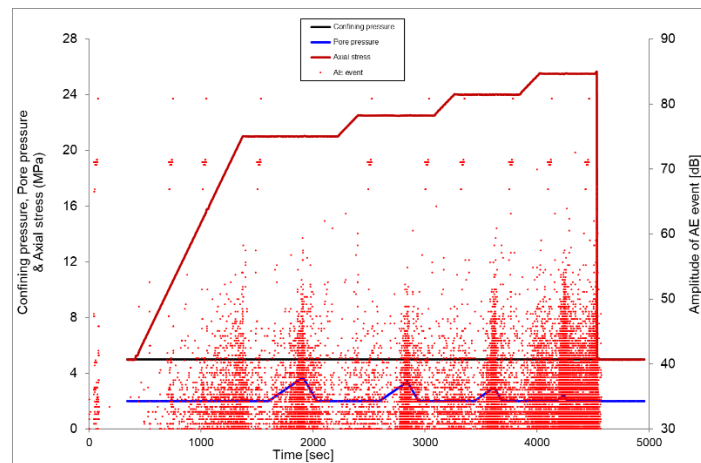


Figure 7. Reactivation of the fracture in a small sample test on Castlegate sandstone. Significant increase in AE is seen (red dots) as the pore pressure is increased (blue line) while the applied stresses are kept constant (Cerasi, not published).

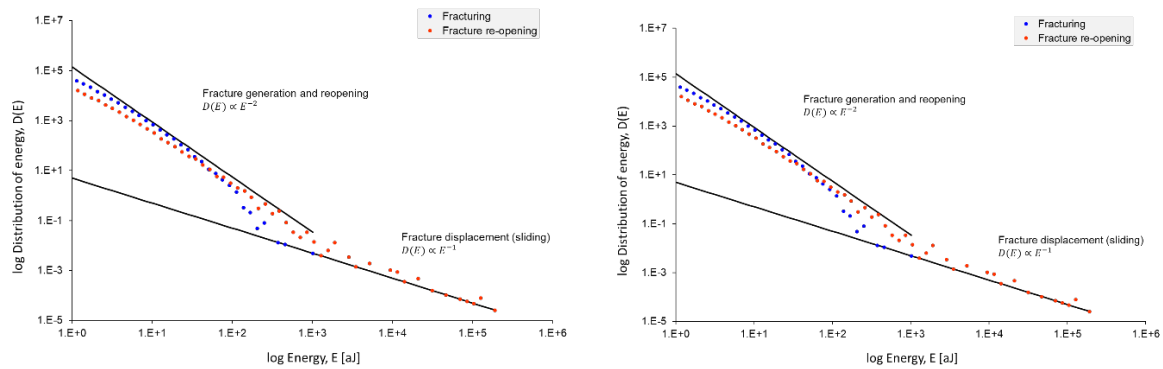


Figure 8. Different scaling law for fracturing and reopening, compared to sliding of fracture (Cerasi, unpublished).

Localisation of the emitted energy is possible, provided the sandstone used is relatively isotropic in terms of ultrasonic velocity (Figure 9). Care has to be taken to calibrate the velocity values to the level of stress; this was done by firing one of the acoustic sensors with a short pulse, recorded by the other sensors, giving a measure of the travel time at various stages of the experiment and hence the velocity at that stress level. At the end of the tests, micro-CT scans can be carried out confirming the accuracy of the localisation (Figure 10).

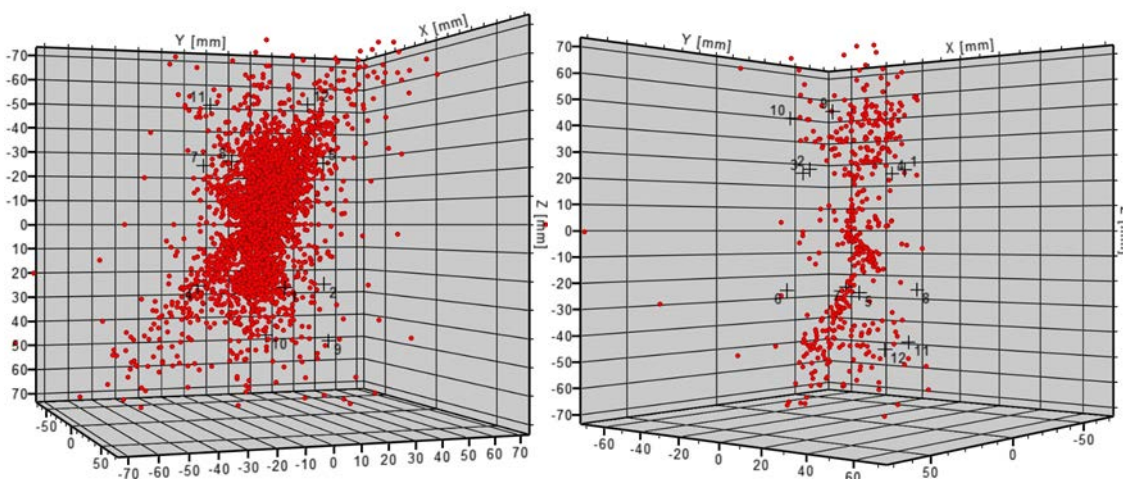


Figure 9. Localisation of AE events in Mt. Simon sandstone (left) and Castlegate outcrop (right). From Cerasi et al., 2018.



Figure 10. Micro-CT image reconstruction isolating the fracture planes detected in the two sandstone specimens with stress-induced fractures. Left: Mt. Simon sandstone; right: Castlegate sandstone (Cerasi *et al.*, 2018).

Compared to the stress-induced fracture tests, in tests conducted on pre-cut (saw-cut) sandstone plugs, no AE was recorded in the small specimens and no large strain occurred upon increase of the pore pressure until the differential stress was significantly increased and when a ~5 times increase in pore pressure was applied (Figure 11) (Cerasi *et al.*, 2018). In the large, cubic meter, true triaxial test of Oye *et al.*, 2018, no significant reactivation occurred prior to hydraulically fracturing the rock; the new fracture connected to the saw-cut plane and reactivated it. Again, true triaxial tests do not reflect the downhole situation exactly, as liquid is injected into a dry sandstone in the laboratory, while in the field, the sandstone is brine saturated.

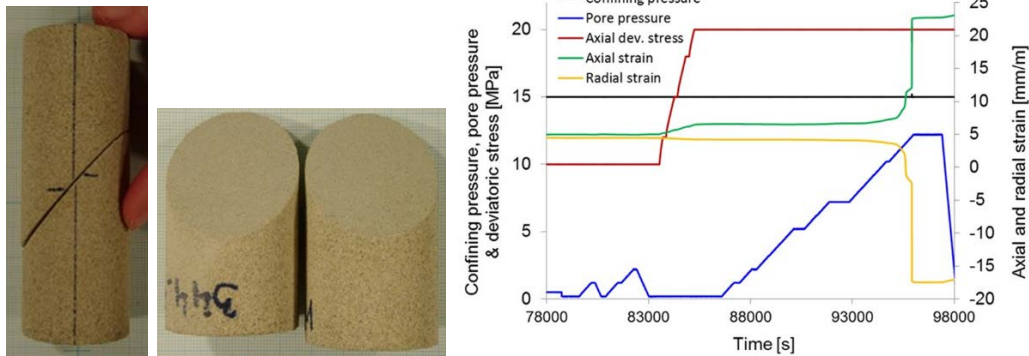


Figure 11. Left: Castlegate sandstone plug cut in two parts, reassembled in the triaxial cell to form a pre-existing fracture (Cerasi, unpublished). Typical test result (no AE recorded) showing reactivation only happened for high deviatoric stress and high pore pressure increase (large drop/increase in radial/axial strain).

The advantage of the stress-induced fracture tests is that the failure plane is "automatically" oriented in the most critical angle for further reactivation (provided the stress path is not changed). The saw-cut samples had a predetermined orientation, which for practical reasons of avoiding the loading pistons, restricted the possible angles, probably making the artificial fault not critically oriented. This would explain the delay in reactivation/slip of the fault. Also, the saw-cut fractures had no history of prior shear as in the case of the stress-induced fracture; under confining stress buildup they closed almost completely, which is reflected by the almost intact cohesion of the reassembled plug. Thus, these fractures were not "reactivated" but simply sheared once the stress conditions were sufficiently high.



2.3 PLANNED TESTS IN THE SECURE PROJECT

AE tests are planned to be conducted at SINTEF's Formation Physics laboratory, whereby energy distribution will be recorded for different size rock specimens. The goal of these tests will be to help upscale the fracturing acoustic signatures to field scales, such that their predictive accuracy can be improved. Size effect is a known laboratory artefact that leads to changing the mechanical strength values found in experiments on rocks; basically, smaller specimens are stronger than larger ones from the same lithology, hollow cylinder specimens get stronger the smaller the borehole (Papamichos & Van den Hoek, 1995). Size effect also comes into play via the cylindrical plug's outer boundary, in mechanical tests including fracture propagation from a borehole or shear failure of the borehole followed by flow-driven erosion (Papamichos *et al.*, 2008). As already mentioned, when the fracture or erosion slit comes nearer the outer surface, stress concentration leads to earlier breakthrough for small specimens compared to larger ones (Figure 5).

This increase in stress leading to accelerating fracture propagation, will be reflected by increased acoustic activity for the smaller samples, at constant hydraulic fracture pressure. It may turn out that this effect reduces the emission activity relative to the time to failure of the outer boundary. Alternatively, attenuation of the acoustic signals will mean less energy will be recorded at the early stages on the larger samples, because the receiving sensors are on the outer surface of the plugs. Therefore, the anticipated useful results of the planned tests will be the presence or absence, and hopefully type of, specific upscaling law of laboratory AE signals to field conditions.

The AE tests will be performed on sandstone and shale outcrop specimens, such as the Castlegate sandstone and the Mancos shale, using plug diameters of several sizes (depending on possibility of rubber sleeve manufacture, from 1" up to 8"). A central axially drilled borehole will be used to pressurise high-viscosity silicon oil (alternately, a glycerol in water solution), to induce the fracture. A combination of passive and active seismic will allow for calibrated AE monitoring of the tests, with analyses of the ensuing emitted energy versus The number of AE events. For sandstone specimens, tests will be repeated without borehole injection, using instead the pore pressure increase on stress-induced fracture method, of relevance for the CCS case.

3 Recommendations for mitigating seismicity

Based on the results of laboratory AE tests, it seems that some mitigation strategies would be worth testing at larger scale. One could for example closely monitor precursors to hydraulic fracturing with downhole acoustic sensors such as DAS cables, when the well pressure is slowly increased; this supposes that some shear deformation occurs around the borehole, due to rock heterogeneity and completion geometry (presence of cement sheath and perforations). If initial microcracking can be recorded, one could simply hold the well pressure at this constant level, or alternatively cycle it up and down from or around this value to induce fatigue and stress corrosion. Once an initial fracture is thus obtained, it is speculated that reopening and further propagation could be obtained at lower well pressure and with less acoustic energy release. For the CCS case, the same strategy could set limits on injection rates, by again listening to the first micro-cracks and reducing slightly the injection pressure to ensure lower magnitudes in the continuation of operations.

However, more laboratory testing is needed to confirm the viability of such well-based strategies to mitigate AE emission. Such tests should look at specific geometry variations and the presence of well completion materials for the case of hydraulic fracturing (Figure 12). For the case of CCS operations, the coupling to basement rock with its own fractures seems to be important and should be reproduced somehow in laboratory investigations. A complicating factor is also the possible presence of variously oriented natural fractures: interaction of induced fractures with the natural fractures could produce additional AE which is not predictable from the initial fracture energy release levels.

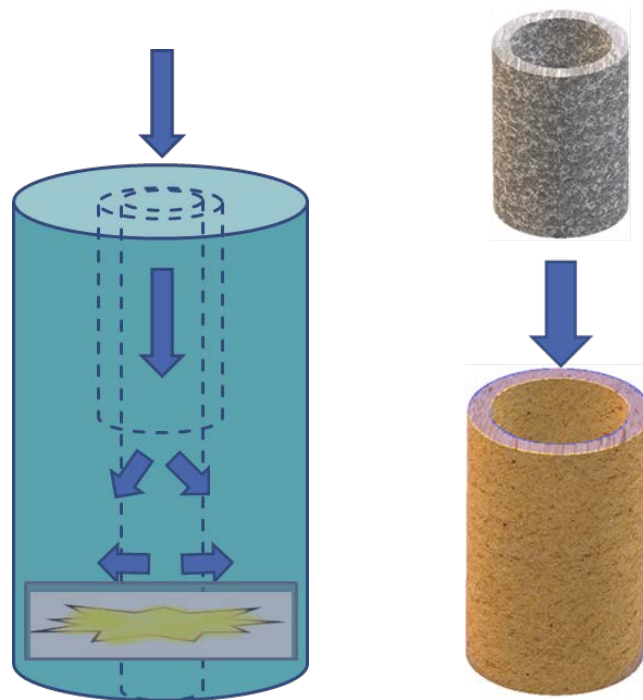


Figure 12 Schematic illustration of planned fracturing experiments to test remediation fluid placement and property evaluation. At left: a shale core with a partially cemented borehole section is fractured by pressurising the borehole. Right: geometry of the assembly showing the cement sheath covering part of the internal surface area of the borehole.

4 Conclusions

In this short report, we have reviewed the state-of-the-art in AE testing in the laboratory, emphasising tests performed at SINTEF in recent years with the aim to investigate conditions where a pore pressure increase corresponding to injection of CO₂ in the field can reactivate a fault and in so doing cause microseismicity. Regarding shale gas applications, AE tests in the laboratory try to replicate at small scale the process of hydraulic fracturing from a pressurised well. This can be done with no fluid communication from the well (pressure from the well pushes a bladder against the formation) or with (viscous) fluid invading dry porous rock (most experiments in the literature). Few, if any, experiments have had fluid invading an anisotropic shale with controlled pore pressure.

The planned experiments in the SECURE project will be designed to address some of the above issues: check correct up-scaling of AE experiments by repeating them at several plug diameters, assess the presence of cement and perforations on the propagation of a hydraulic fracture and perform AE tests on low permeability shale plugs.

Some remediation recommendations are put forward using the concept of stress corrosion, highlighted in fatigue experiments with AE. It is however too soon to put much confidence in such recommendations as more dedicated laboratory testing is needed to verify the assumptions behind these hypotheses.



5 References

- AKER, E., KÜHN, D., VAVRYČUK, V., SOLDAL, M., OYE, V. (2014). Experimental investigation of acoustic emissions and their moment tensors in rock during failure. *International journal of rock mechanics and mining sciences*, 70, 286-295.
- BACCI, V. O., TAN, J., HALLADAY, A., & O'BRIEN, S. (2018). Microseismic activity after 2+ years of CO₂ injection at Quest. In *SEG Technical Program Expanded Abstracts 2018* (pp. 3052-3056).
- BAUD, P., KLEIN, E., WONG, T.-F. Compaction localization in porous sandstones: spatial evolution of damage and acoustic emission activity. *Journal of Structural Geology*, 26 (2004) 603–624.
- BUNGER, A.P., KEAR, J., JEFFREY, R.G., PRIOUL, R., CHUPRAKOV, D. Laboratory investigation of hydraulic fracture growth through weak discontinuities with active ultrasound monitoring. *Innovations in Applied and Theoretical Rock Mechanics Editors – Hassani, Hadjigeorgiou, Archibald*. ©2015 by the Canadian Institute of Mining, Metallurgy & Petroleum and ISRM, ISBN 978-1-926872-25-4.
- BUTCHER, A., LUCKETT, R., VERDON, J. P., KENDALL, J. M., BAPTIE, B., WOOKEY, J. (2017). Local magnitude discrepancies for near-event receivers: Implications for the UK traffic-light scheme. *Bulletin of the Seismological Society of America*, 107(2), 532-541.
- CERASI, P., STROISZ, A., SØNSTEBØ, E., STANCHITS, S., OYE, V., BAUER, R. (2018). Experimental investigation of injection pressure effects on fault reactivation for CO₂ storage. *International Journal of Greenhouse Gas Control*, 78, 218-227.
- CHEN, P., RAHMAN, M. M., & SARMA, H. K. (2014, November). Interaction between hydraulic fracture and natural fracture—a new prediction model by adaptive neuro-fuzzy inference system (ANFIS). In *Abu Dhabi International Petroleum Exhibition and Conference*. Society of Petroleum Engineers.
- CHENG, Y. (2012). Impact of water dynamics in fractures on the performance of hydraulically fractured wells in gas-shale reservoirs. *Journal of Canadian Petroleum Technology*, 51(02), 143-151.
- CHITRALA, Y., MORENO, C., SONDERGELD, C., RAI, C. An experimental investigation into hydraulic fracture propagation under different applied stresses in tight sands using acoustic emissions. *Journal of Petroleum Science and Engineering*, 108 (2013), pp.151–161.
- DAHI-TALEGHANI, A., OLSON, J. E. (2011). Numerical modeling of multistranded-hydraulic-fracture propagation: accounting for the interaction between induced and natural fractures. *SPE journal*, 16(03), 575-581.
- DANDO, B. D. E., GOERTZ-ALLMANN, B., IRANPOUR, K., KÜHN, D., OYE, V. (2019). Enhancing CO₂ monitoring at the Decatur CCS site through improved microseismic location constraints. In *SEG Technical Program Expanded Abstracts 2019* (pp. 4893-4897).
- ELIASSON, P., CERASI, P., ROMDHANE, A., SCHMIDT-HATTENBERGER, C., CARPENTIER, S., GRIMSTAD, A. A., LOTHE, A. (2018, October). Pressure control and conformance management for safe and efficient CO₂ storage – an overview of the Pre-ACT project. In *14th Greenhouse Gas Control Technologies Conference Melbourne*, pp. 21-26.
- FORTIN, J., STANCHITS, S., DRESEN, G., GUÉGUEN, Y. Acoustic emission and velocities associated with the formation of compaction bands in sandstone. *Journal of Geophysical Research*, vol. 111, b10203, doi:10.1029/2005JB003854, 2006.
- FORTIN, J., STANCHITS, S., DRESEN, G., GUÉGUEN, Y. Acoustic Emissions Monitoring during Inelastic Deformation of Porous Sandstone: Comparison of Three Modes of Deformation. *Pure appl. geophys.*, 166 (2009) 823–841.
- GOERTZ-ALLMANN, B. P., JORDAN, M., BAUER, R., OYE, V., GREENBERG, S. E. (2017, August). Integrating Active with Passive Seismic Data to Best Constrain CO₂ Injection Monitoring. In *EAGE/SEG Research Workshop 2017*.
- GRUDE, S., LANDRØ, M., & DVORKIN, J. (2014). Pressure effects caused by CO₂ injection in the Tubåen Fm., the Snøhvit field. *International Journal of Greenhouse Gas Control*, 27, 178-187.
- LOCKNER, D. The role of acoustic emission in the study of rock fracture. *Int. J. Rock Mech. Min. Sci. & Geomech. Abstr.* Vol.30, No.7, pp. 883-899, 1993.
- MATSUNAGA, I., KOBAYASHI, H., SASAKI, S., ISHIDA, T. Studying Hydraulic Fracturing Mechanism by Laboratory Experiments with Acoustic Emission Monitoring. *Int. J. Rock Mech. Min. Sci. & Geomech. Abstr.* Vol.30, No.7, pp. 909-912, 1993.
- MCLASKEY, G.C., LOCKNER, D.A. Calibrated Acoustic Emission System Records M -3.5 to M -8 Events Generated on a Saw-Cut Granite Sample. *Rock Mech Rock Eng.* (2016) 49:4527–4536.
- MOLEND, M., STÖCKHERT, F., BRENNE, S., ALBER, M. Acoustic Emission monitoring of laboratory scale hydraulic fracturing experiments. ARMA 15-69. *49th US Rock Mechanics / Geomechanics Symposium, San Francisco, CA, USA*, 28 June-1 July 2015.



- OYE, V., STANCHITS, S., SEPRODI, N., CERASI, P., STROISZ, A.M., BAUER, R. (2018, June). Dynamics of Stick-Slip Sliding Induced by Fluid Injection in Large Sandstone Block. In *80th EAGE Conference and Exhibition 2018*.
- PAPAMICHOS, E., J.F. STENEBRÅTEN, P. CERASI, A. LAVROV, I., VARDOLAKIS, G.F. FUH, M. BRIGNOLI, C.J. GONÇALVES DE CASTRO, AND O. HAVMØLLER. 2008. Rock type and hole failure pattern effects on sand production. In *Proceedings of the 42nd US Rock Mechanics Symposium and 2nd US-Canada Rock Mechanics Symposium, San Francisco, California, USA, 29 June-2 July 2008*, ARMA 08-217.
- PAPAMICHOS, E., VAN DEN HOEK, P. Size dependency of Castlegate and Berea sandstone hollow-cylinder strength on the basis of bifurcation theory. *Proc. 35th US Symp. Rock Mechanics*. Rotterdam, Netherlands: Balkema, 1995. p. 301-306.
- PRADHAN, S., STROISZ, A.M., FJÆR, E., STENEBRÅTEN, J.F., LUND, H.K., SØNSTEBØ, E.F. (2015). Stress-induced fracturing of reservoir rocks: acoustic monitoring and μ CT image analysis. *Rock Mechanics and Rock Engineering*, 48 (6), 2529-2540.
- RINGROSE, P., GREENBERG, S., WHITTAKER, S., NAZARIAN, B., & OYE, V. (2017). Building confidence in CO₂ storage using reference datasets from demonstration projects. *Energy Procedia*, 114, 3547-3557.
- SMITH, J. D., WHITE, R.S., COPLEY, A., AVOUAC, J.P., GUALANDI, A. (2017, December). Subsidence and Seismicity in the Groningen Region, North-East Netherlands. In *AGU Fall Meeting Abstracts*.
- STANCHITS, S., SURDI, A., GATHOGO, P., EDELMAN, E., SUAREZ-RIVERA, R. (2014). Onset of Hydraulic Fracture Initiation Monitored by Acoustic Emission and Volumetric Deformation Measurements. *Rock Mech Rock Eng*, (2014) 47:1521–1532, DOI 10.1007/s00603-014-0584-y.
- SUN, X. Z., SHEN, B., ZHANG, B. L. (2018). Experimental study on propagation behavior of three-dimensional cracks influenced by intermediate principal stress. *Geomechanics and Engineering*, 14(2), 195–202. <https://doi.org/10.12989/GAE.2018.14.2.195>.
- SZWEDZICKI, T. (2001). Geotechnical precursors to large-scale ground collapse in mines. *International Journal of Rock Mechanics and Mining Sciences*, 38(7), 957-965.
- WANG, J., XIE, L., XIE, H., REN, L., HE, B., LI, C., YANG, Z., GAO, C. Effect of layer orientation on acoustic emission characteristics of anisotropic shale in Brazilian tests. *Journal of Natural Gas Science and Engineering*, 36 (2016) 1120e1129.
- WINNER, R.A., LU, G., PRIOUL, R., AIDAGULOV, G., BUNGER, A.P. Acoustic emission and kinetic fracture theory for time-dependent breakage of granite. *Engineering Fracture Mechanics*, 199 (2018) 101–113.